Materials Science and Engineering A 528 (2011) 7715–7722

Contents lists available at ScienceDirect

Materials Science and Engineering A

journal homepage: www.elsevier.com/locate/msea

Microstructural evolution and mechanical properties of a Cu–Zr alloy processed by high-pressure torsion

Jittraporn Wongsa-Ngam [a], Megumi Kawasaki [a,*], Yonghao Zhao [b], Terence G. Langdon [a,c]

[a] Departments of Aerospace & Mechanical Engineering and Materials Science, University of Southern California, Los Angeles, CA 90089-1453, USA
[b] Department of Chemical Engineering and Materials Science, University of California, Davis, CA 95616, USA
[c] Materials Research Group, School of Engineering Sciences, University of Southampton, Southampton SO17 1BJ, UK

ARTICLE INFO

Article history:
Received 24 May 2011
Received in revised form 17 June 2011
Accepted 18 June 2011
Available online 24 June 2011

Keywords:
Copper alloy
Hardness
High-pressure torsion
Homogeneity
Ultrafine grains

ABSTRACT

Experiments were conducted on a Cu–0.1% Zr alloy in order to examine the evolution of hardness and microstructure after processing by high-pressure torsion. Disks were pressed through different numbers of revolutions up to a maximum of 10 turns using an applied pressure of 6.0 GPa. It is shown that there is a gradual evolution in both the hardness and the microstructure with increasing numbers of turns. After 5 and 10 turns there is a high degree of hardness homogeneity and the microstructure consists of well-defined equiaxed grains. The measured grain size after 5 turns was ~180 nm in the peripheral region of the disk. Tensile testing at 673 and 723 K after processing through 5 and 10 turns showed a maximum elongation to failure of ~280% at 723 K using a strain rate of 1.0×10^{-4} s^{-1}.

1. Introduction

Equal-channel angular pressing (ECAP) [1] and high-pressure torsion (HPT) [2] are two processing techniques that are used to introduce very significant grain refinement into bulk metals. Typically, the grain sizes produced by these techniques are within the submicrometer (0.1–1.0 μm) or even the nanometer (<100 nm) range. The experimental evidence available to date shows that processing by HPT leads to average grain sizes that are smaller than those produced by ECAP [3–5] and accordingly HPT is an especially attractive process for evaluating the development of highly refined microstructures.

Earlier experiments on aluminum-based alloys, conducted using ECAP, demonstrated that the addition of a small amount of Zr was effective in inhibiting grain growth at elevated temperatures [6,7] and it was further shown that a Zr addition provides a potential for achieving superplastic elongations of up to >1000% when conducting tensile tests at high temperatures [8]. Similar experiments were also conducted on pure Cu and Cu alloys and it was demonstrated that a Zr addition leads to a significant increase in the recrystallization temperature [9]. Nevertheless, although superplastic elongations were achieved with a Cu–30% Zn–0.13% Zr alloy after processing by ECAP and testing at a temperature of 673 K, similar experiments on a Cu–0.18% Zr alloy were less successful and the elongations to failure were consistently <100% over a range of strain rates [9].

To date, there appear to be no similar experiments on Cu–Zr alloys processed by HPT although it is well established that a Zr addition is important in Cu because it improves the fatigue life [10]. Accordingly the present research was initiated with two specific objectives. First, to apply HPT processing to samples of pure Cu containing a minor addition of Zr in order to evaluate the consequent microstructural evolution both throughout each disk and with increasing torsional strain. Second, to evaluate the high temperature mechanical properties after HPT processing and especially to examine the feasibility of achieving a true superplastic behavior.

2. Experimental materials and procedures

The experiments were conducted using a commercial Cu151 alloy having a composition, in wt.%, of Cu–0.1% Zr. The alloy was received from Olin Brass (East Alton, IL, USA) in the form of a rolled strip with dimensions of 760 × 500 mm and a thickness of 1.5 mm. Disks were punched from the strip with diameters of 10 mm and they were polished to final thicknesses of ~0.83 mm. In the as-received condition, the mean linear intercept grain size was ~20 μm.

The HPT processing was conducted under quasi-constrained conditions [2] using a facility consisting of upper and lower anvils having central depressions with diameters of 10 mm and depths of 0.25 mm: these depressions were used to hold each disk in place during torsional straining. The processing procedure was described

* Corresponding author. Tel.: +1 213 740 4342; fax: +1 213 740 8071.
E-mail address: mkawasak@usc.edu (M. Kawasaki).

0921-5093/$ – see front matter © 2011 Elsevier B.V. All rights reserved.
doi:10.1016/j.msea.2011.06.056

earlier [11] except that a lubricant was not placed around the edges of the depressions on the upper and lower anvils. Each disk was processed at room temperature by rotating the lower anvil at a speed of 1 rpm under an applied load of ~470 kN corresponding to an imposed compressive pressure, P, of 6.0 GPa. Separate disks were processed through totals of $N = 1/4$, 1/2, 1, 3, 5 and 10 turns.

Following HPT, the mechanical characteristics were evaluated by measuring the microhardness and tensile properties. Each processed disk was mounted and polished to have a mirror-like surface quality and microhardness measurements were taken using an FM-1e microhardness tester equipped with a Vickers indenter. All measurements of the Vickers microhardness, Hv, were recorded using a load of 200 gf and a dwell time of 10 s. Two different procedures were used for these measurements as described in an earlier report [11]. First, the average microhardness values were measured along a randomly selected diameter of each disk. These measurements were taken at intervals of 0.3 mm and at every point the local value of Hv was taken as the average of four separate hardness values recorded at uniformly separated points displaced from the selected point by a distance of 0.15 mm. Using this procedure, it was possible to achieve a high accuracy in the individual values of Hv and for every position the error bars were estimated corresponding to the 95% confidence limits. Second, the distribution of local hardness was measured over the total surface of each individual disk by recording the individual values of Hv following a rectilinear grid pattern with an incremental spacing of 0.3 mm. These individual datum points were then used to construct color-coded contour maps to provide a simple visual display of the hardness distributions within each disk.

The tensile properties were evaluated after HPT processing through 5 and 10 turns. Two miniature tensile specimens were cut from each disk using electro-discharge machining (EDM). These tensile specimens had gauge lengths and widths of 1 mm and they were cut from off-center positions in the HPT disks to avoid any potential problems associated with microstructural inhomogeneities near the disk centers: an earlier report provided a schematic illustration of a typical tensile specimen [12]. The tensile samples were pulled to failure at temperatures of 673 and 723 K using a testing machine operating at a constant rate of cross-head displacement with initial strain rates from 1.0×10^{-4} to $1.0 \times 10^{-2}\ s^{-1}$.Specimens were prepared for examination by transmission electron microscopy (TEM) by punching 3 mm diameter disks from the center and edge regions of selected disks, mechanically grinding to thicknesses of <50 μm and then dimpling from both sides to a thickness of ~10 μm. To achieve a high level of electrical transparency, further thinning was performed using a Gatan PIPS 691 ion milling system at a voltage of 4 kV. Bright field images of each sample were taken on a Philips CM12 TEM at a voltage of 100 kV. These observations were used to determine both the fractional distributions of different grain sizes and the average grain size for each processing condition.

3. Experimental results

3.1. Microhardness measurements after HPT

The values of the Vickers microhardness were recorded across the diameter of each disk after HPT processing and the results are shown in Fig. 1 where the values of Hv are plotted along each linear traverse: the lower dashed line denotes the hardness value in the as-received condition prior to processing. For clarity, the individual error bars are not included on the individual points in Fig. 1.

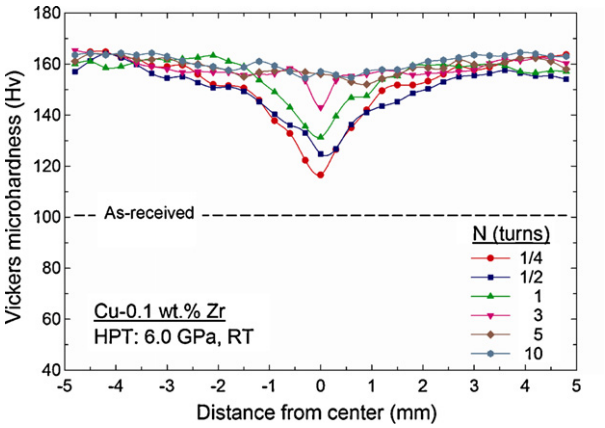

Fig. 1. Values of the Vickers microhardness versus distance from the center of the Cu–0.1% Zr disks after HPT processing for various numbers of turns.

Inspection of Fig. 1 shows the hardness at the edge of the disk increases significantly after 1/4 turn such that there is an increase by a factor of >1.5 by comparison with the as-received condition. By contrast, the hardness in the center of the disk increases only from Hv ≈ 100 to Hv ≈ 120. Thereafter, the hardness values at the peripheries of all disks remain reasonably constant at Hv ≈ 160 and there is no significant increase even up to $N = 10$ turns. By contrast, the hardness values in the centers increase with increasing torsional straining up to $N = 3$ turns and after 5 and 10 turns the hardness values at the centers of the disks are essentially identical to those in the peripheral regions. These results demonstrate the development of a gradual hardness homogeneity across the disks with increasing torsional straining. Detailed information on the values of Hv and the associated error bars are summarized in Table 1 where the error bars denote the 95% confidence limits based on the separate measurements recorded around each point. Excluding the central position at 0 mm, it should be noted that each hardness value is listed at distances from the center of 0.3–4.8 mm and this represents an average of the two separate hardness values recorded on either side of the center and plotted in Fig. 1.

It is apparent from Table 1 that the values of hardness in the centers of the disks are significantly lower than at the edges for up to 3 turns of HPT but thereafter, at 5 and 10 turns, all values of Hv are reasonably consistent. In the early stages of processing, as at $N = 1/4$ turn, the error bars tend to be large across the diameter of the disk but at larger strains, as at $N = 10$ turns, the error bars are consistently low and essentially negligible. These measurements confirm the increasing stability and homogeneity of the hardness distributions across the diameters of the disks.

Using the microhardness values recorded following a rectilinear grid pattern, color-coded contour maps were constructed for $N = 1/4$. 1, 5 and 10 turns: these maps are shown in Fig. 2 where the external coordinates labeled X and Y denote two arbitrary and randomly selected orthogonal axes that are superimposed on the disks such that the center of each disk has a coordinate of (0,0). For all maps, the individual values of Hv are presented as a set of unique colors that cover hardness values from 110 to 170 in incremental steps of 10: the significance of these colors is denoted by the color key on the right in Fig. 2.

In the very early stages of HPT processing through $N = 1/4$ turn in Fig. 2(a), there is a relatively large area of lower hardness confined within the central region of the disk and extending outwards through a diameter of ~4 mm. For this condition, the hardness values reveal significant inhomogeneity. Increasing the straining to $N = 1$ turn decreases the diameter of the central region of lower hardness to ~2 mm as shown in Fig. 2(b) and this central region is

Table 1
Microhardness values along the radii of Cu–0.1% Zr disks processed by HPT.

Distance from center (mm)	Hv					
	1/4 turn	1/2 turn	1 turn	3 turns	5 turns	10 turns
0	116.5 ± 4.6	124.8 ± 5.3	131.3 ± 8.2	143.0 ± 4.6	156.0 ± 4.2	157.0 ± 0.9
0.3	124.4 ± 4.4	129.9 ± 4.4	137.5 ± 4.9	153.5 ± 3.8	156.0 ± 2.4	155.8 ± 0.9
0.6	133.9 ± 4.1	136.1 ± 1.9	144.9 ± 3.3	156.8 ± 2.5	155.1 ± 2.0	154.8 ± 0.7
0.9	139.9 ± 2.7	140.6 ± 2.0	148.3 ± 2.7	156.1 ± 1.3	154.6 ± 2.5	157.0 ± 0.7
1.2	147.6 ± 3.0	144.4 ± 1.5	153.9 ± 1.6	156.6 ± 0.6	155.5 ± 2.0	157.8 ± 0.5
1.5	151.1 ± 1.8	147.3 ± 2.5	157.1 ± 2.0	156.4 ± 1.3	155.4 ± 1.2	157.8 ± 0.4
1.8	151.6 ± 2.3	149.8 ± 1.3	160.1 ± 1.7	156.3 ± 1.5	158.0 ± 1.4	159.3 ± 0.6
2.1	152.6 ± 1.5	150.5 ± 0.8	161.4 ± 1.7	156.5 ± 1.0	158.5 ± 1.2	161.0 ± 0.5
2.4	156.0 ± 1.9	152.9 ± 1.8	161.1 ± 1.4	156.8 ± 1.0	159.1 ± 1.3	161.5 ± 0.7
2.7	159.3 ± 1.0	155.0 ± 1.3	160.5 ± 1.8	156.9 ± 1.5	160.9 ± 0.9	162.5 ± 0.4
3.0	158.4 ± 1.8	155.0 ± 0.6	160.5 ± 1.2	157.9 ± 1.0	161.5 ± 0.7	163.5 ± 0.3
3.3	159.0 ± 2.7	156.3 ± 1.4	161.0 ± 1.6	159.6 ± 1.2	160.6 ± 2.5	163.3 ± 0.2
3.6	161.3 ± 2.7	158.6 ± 1.6	160.0 ± 2.0	161.0 ± 1.7	161.3 ± 2.3	163.3 ± 0.5
3.9	162.3 ± 2.1	159.5 ± 2.4	158.0 ± 2.1	162.3 ± 1.4	162.9 ± 1.5	164.5 ± 0.2
4.2	163.8 ± 2.0	159.6 ± 3.5	157.5 ± 1.2	163.0 ± 0.8	163.0 ± 1.2	164.0 ± 0.4
4.5	163.9 ± 2.6	158.3 ± 2.7	159.1 ± 1.5	163.1 ± 1.5	162.5 ± 2.3	163.0 ± 0.4
4.8	163.7 ± 5.1	155.5 ± 2.4	158.3 ± 1.5	162.4 ± 2.6	159.0 ± 2.0	163.0 ± 0.2

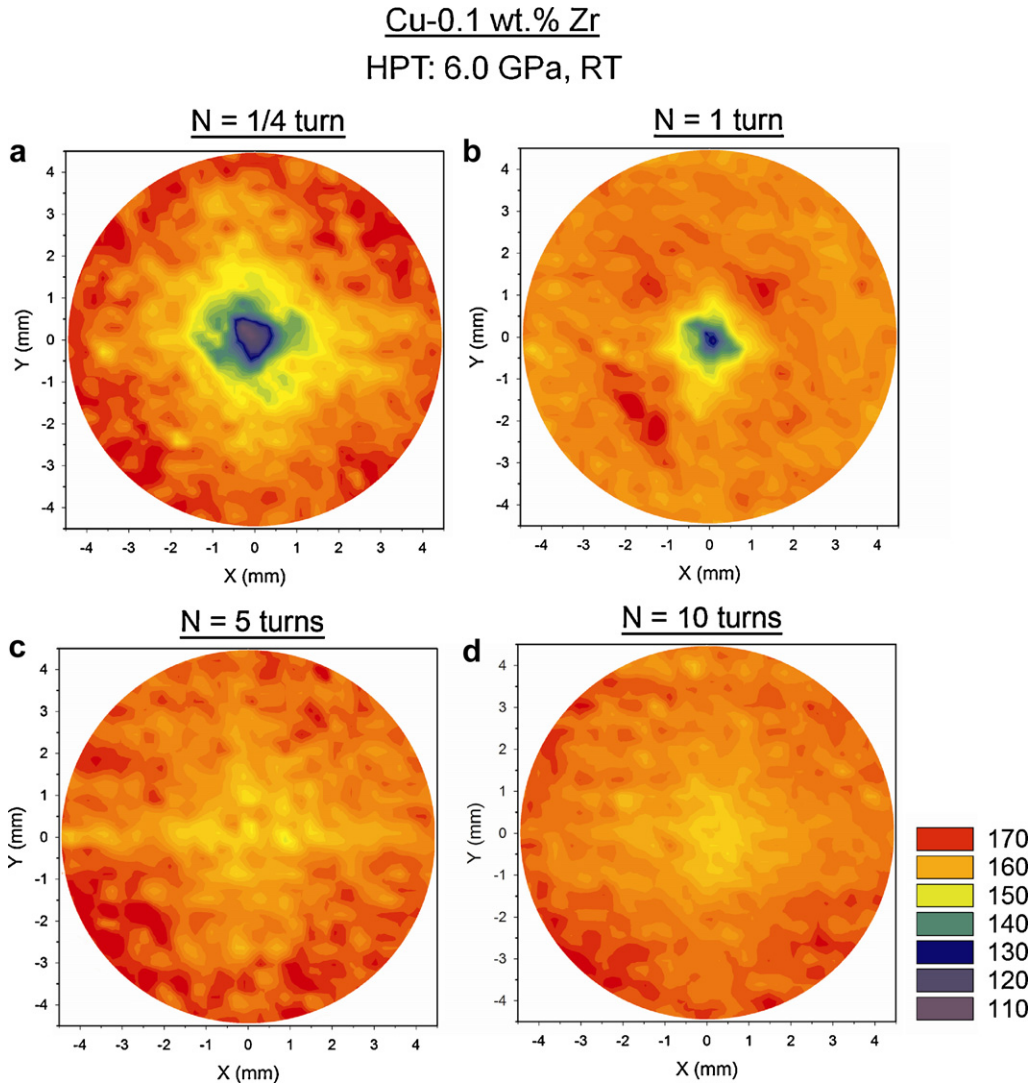

Fig. 2. Color-coded contour maps showing the distributions of the Vickers microhardness values over disks processed by HPT at a pressure of 6.0 GPa for (a) 1/4 turn, (b) 1 turn, (c) 5 turns and (d) 10 turns. (For interpretation of the references to color in this figure legend, the reader is referred to the web version of the article.)

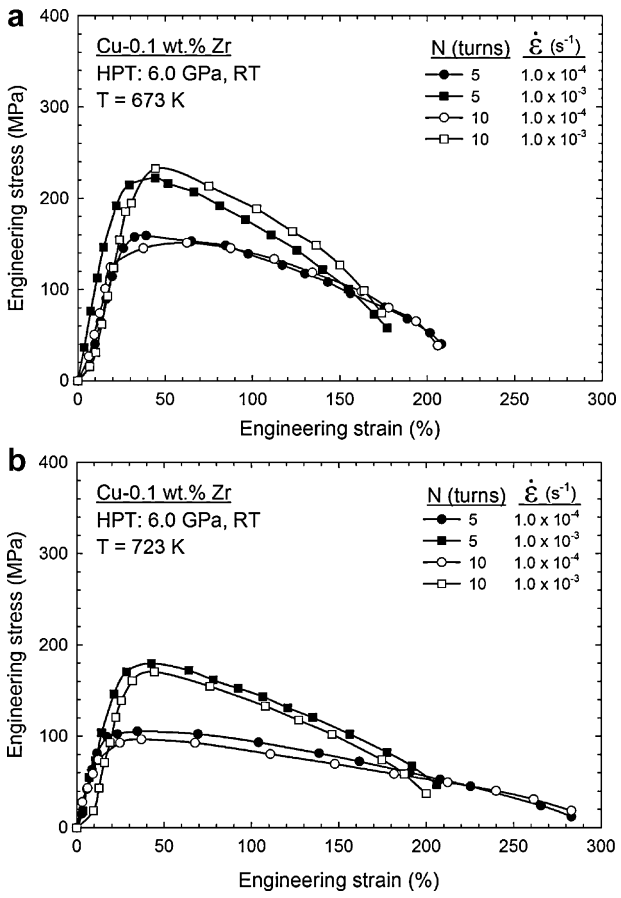

Fig. 3. Plots of engineering stress versus engineering strain for the Cu–0.1% Zr alloy processed through 5 and 10 turns of HPT and pulled to failure at different initial strain rates at (a) 673 and (b) 723 K.

essentially removed after HPT through 5 and 10 turns as shown in Fig. 2(c) and (d). Since the disks processed through 5 and 10 turns show similar hardness distributions over the entire disk surfaces, these hardness measurements suggest that a reasonably homogeneous hardness may be attained in the Cu–0.1% Zr alloy by HPT processing at room temperature through $N = 5$ turns under a pressure of $P = 6.0$ GPa. The present results were achieved using an anvil rotation speed of 1 rpm but earlier results with a magnesium AZ31 alloy show the rotation speed has only a minor effect on the processed microstructure [13].

3.2. Mechanical properties at high temperatures

The hardness measurements indicate that HPT processing through 5 or more turns is sufficient to achieve a reasonably uniform hardness distribution throughout the disks of the Cu–0.1% Zr alloy. The earlier results on the Cu–30% Zn–0.13% Zr alloy processed by ECAP indicated a potential for achieving superplastic elongations in Cu–Zr alloys at a testing temperature of 673 K and strains rates of 10^{-4} and 10^{-3} s^{-1} [9]. Accordingly, Fig. 3 shows representative stress–strain curves for specimens tested through 5 and 10 turns and tested at strain rates of 1.0×10^{-4} and 1.0×10^{-3} s^{-1} at temperatures of (a) 673 and (b) 723 K. These plots show the Cu–Zr alloy exhibits typical high temperature behavior including little strain hardening and reasonable ductility. It is also apparent that the overall ductility increases with increasing temperature and with decreasing strain rate.

Fig. 4 displays the variation of the elongation to failure with strain rate for the Cu–Zr alloy processed by HPT for 5 and 10 turns and tested at 673 and 723 K. The results are similar at both temperatures with an increase in the elongation to failure with decreasing strain rate. The highest elongations of ~280% were recorded in these experiments for the two specimens processed through $N = 5$ and 10 turns when testing at 723 K under an imposed initial strain rate of 1.0×10^{-4} s^{-1}.

It is apparent from Figs. 3 and 4 that the deformation behavior of the specimens processed by HPT for 5 and 10 turns are essentially identical under all testing conditions. This is consistent with the hardness measurements in Figs. 1 and 2 which show essentially identical hardness values after 5 and 10 turns. It is also consistent with earlier studies demonstrating a close correlation between the individual microhardness measurements and the internal microstructures [14–20]

3.3. Microstructures after processing by HPT

The evolution of microstructure was examined using TEM with disks of the Cu–0.1% Zr alloy processed through $N = 1/4$, 1 and 5 turns. Representative microstructures are shown in Fig. 5 for (a) 1/4 turn, (b) 1 turn and (c) 5 turns, where the upper row corresponds to the centers of the disks and the lower row corresponds to the peripheries of the disks, respectively.

Inspection shows the microstructures in the centers of the disks are similar after 1/4 and 1 turn in the upper row of Fig. 5(a) and (b) where there are indistinct (sub)grain boundaries but also a clear dislocation cell structure. Large numbers of dislocations were observed within the grains for these two samples. At the edge of the disk after 1/4 turn many of the (sub)grain boundaries are not clearly defined but the grains are finer than in the central region. Continuous straining through 1 turn produced reasonably equiaxed grains with sharp boundaries although some larger grains also remained at the edge of the disk as shown in the lower row in Fig. 5(b). Thereafter, the microstructure becomes uniformly finer with equiaxed grains having well-defined grain boundaries in both the central and peripheral regions of the disk after processing through 5 turns of HPT as shown in Fig. 5(c). The well-defined microstructure throughout the disk after HPT for 5 turns is consistent with the hardness measurements shown in Figs. 1 and 2.

Fig. 6 shows histograms of the grain size distributions measured at four different positions: (a) at the peripheral region of the disk after 1/4 turn, (b) at the peripheral region of the disk after 1 turn, (c) at the central region of the disk after 5 turns and (d) at the peripheral region of the disk after 5 turns. In the centers of the disks after 1/4

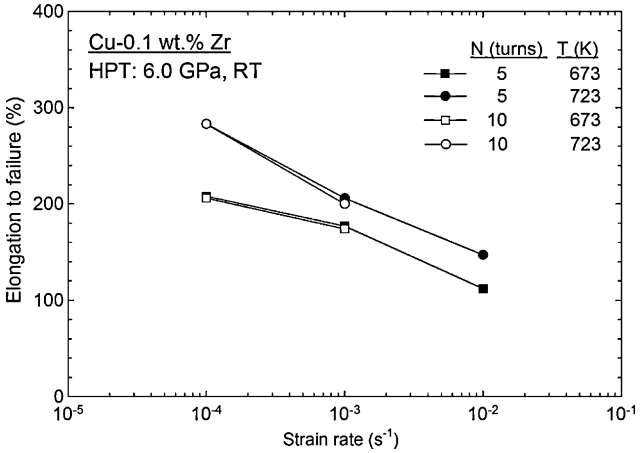

Fig. 4. Elongation to failure versus strain rate for the Cu–0.1% Zr alloy processed by HPT for 5 and 10 turns and tested at 673 and 723 K.

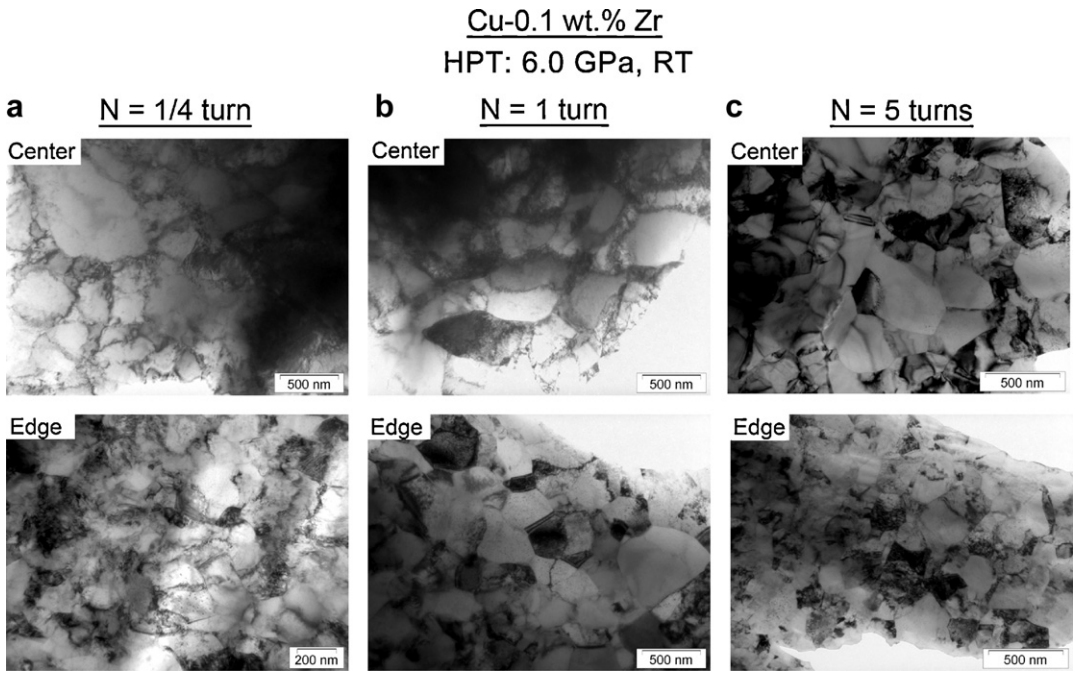

Fig. 5. Representative TEM micrographs of the Cu–0.1% Zr disks processed by HPT for (a) 1/4 turn, (b) 1 turn and (c) 5 turns: the upper row corresponds to the centers of the disks and the lower row corresponds to the edges of the disks.

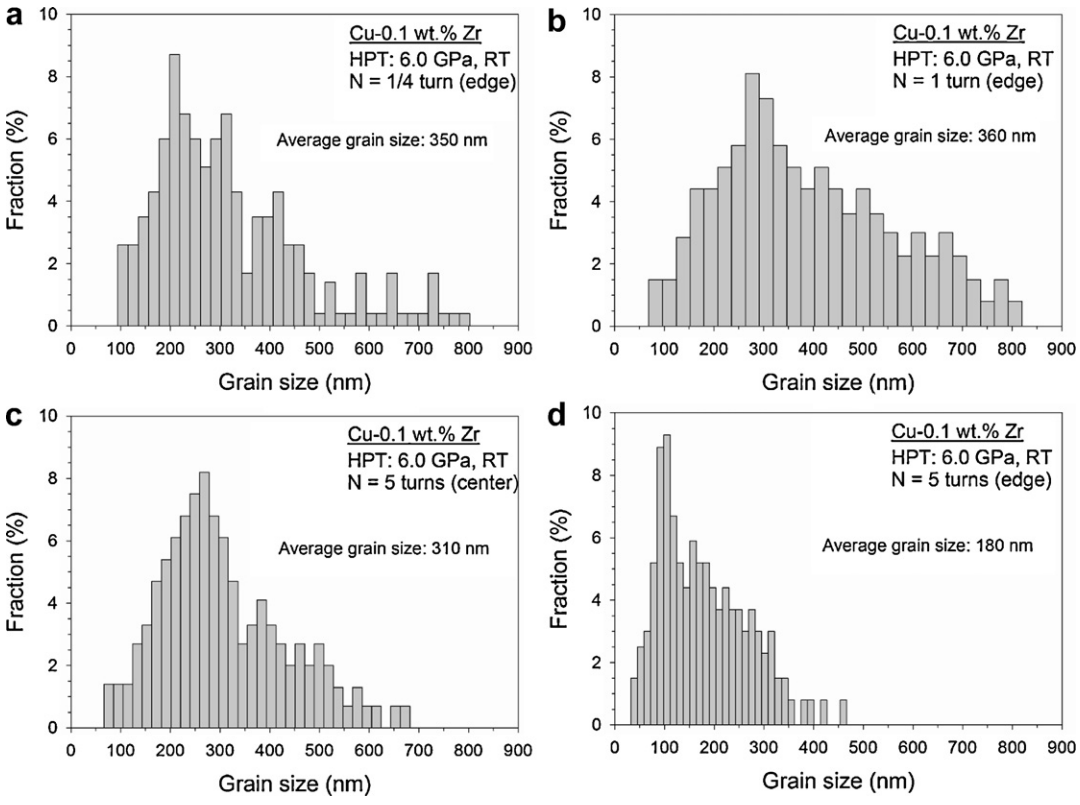

Fig. 6. Histograms of the grain size distributions measured at (a) a peripheral region of the disk after 1/4 turn, (b) a peripheral region of the disk after 1 turn, (c) a central region of the disk after 5 turns and (d) a peripheral region of the disk after 5 turns: the individual average grain sizes are indicated.

and 1 turn, the grains were poorly defined and it was not possible to take quantitative measurements. At the edges of the disks after 1/4 and 1 turn, individual grain sizes were recorded over a wide range from ~100 to ~800 nm and the average grain sizes were measured as ~350–360 nm. Despite the similarity in these two average sizes, there were different peak fractions of ~200 and ~300 nm for the disks processed through 1/4 and 1 turn, respectively, as shown in Fig. 6(a) and (b). This difference arises because of the larger numbers of dislocations observed at most of the grain boundaries at the edge of the disk after 1/4 turn as shown in the lower row in Fig. 5(a).

After 5 turns of HPT, the range of grain sizes was reduced to 80–670 nm with a peak fraction at ~250 nm in the central region and 40–460 nm with a peak fraction at ~100 nm in the peripheral region as shown in Fig. 6(c) and (d). A smaller average grain size of ~180 nm was recorded at the edge of the disk compared with an average size of ~310 nm at the center of the disk after 5 turns. Thus, although the microstructure was reasonably consistent across the disk after 5 turns as shown in the upper and lower rows in Fig. 5(c), and this is similar to the hardness homogeneity recorded in Fig. 2(c) after 5 turns, nevertheless there is a wider distribution of grain sizes in the center of the disk and this leads both to a larger average grain size and, as shown in Table 1, to larger error bars on the hardness measurements recorded in the central region of the disk after 5 turns.

It is evident from the hardness data in Fig. 1 that there is only a small variation in the values of Hv near the edges of the disks from $N = 1/4$ to $N = 5$ turns although the average grain size is reduced with increasing N as shown in Fig. 6(a) and (d). The lack of any significant change in Hv is due to an approximate balance with increasing N between the increase in hardness due to the reduction in the average grain size and the decrease in hardness due to the significant decrease in the dislocation densities at the peripheries of the disks as is apparent from inspection of Fig. 5(a) and (c).

4. Discussion

4.1. Hardness and microstructure evolution in HPT processing

The principle of HPT is relatively simple. When a disk is processed by HPT, the equivalent von Mises strain imposed on the disk, ε_{eq}, is given by a relationship of the form [21–23]:

$$\varepsilon_{eq} = \frac{2\pi N r}{h\sqrt{3}} \quad (1)$$

where r and h are the radius and height (or thickness) of the disk, respectively. It is apparent from Eq. (1) that the imposed strain is a maximum around the edge of the disk whereas it becomes equal to zero in the center of the disk where $r = 0$. In practice, however, Eq. (1) includes only the effect of torsional straining and there is also an additional strain imposed by the compressive pressure, P. Recent experiments on an Al-6061 aluminum alloy showed the initial applied pressure leads to a significant increase in hardness across the disk diameter even in the absence of any torsional straining [24].

It is anticipated from Eq. (1) that the microstructures and microhardness values introduced by HPT will be extremely inhomogeneous. Nevertheless, very early experiments demonstrated a gradual evolution towards a homogeneous structure in disks of Ni processed by HPT by increasing either the applied pressure, P, and/or the total numbers of revolutions, N [4,14]. Subsequently, numerous reports confirmed this gradual evolution towards homogeneity [11,15–20,25–30] and the evolution was successfully modeled using strain gradient plasticity theory [31].

The evolution in hardness values with increasing torsional strain, as shown in Fig. 1, is similar to earlier reports for pure Cu processed by HPT for up to 5–25 turns [26,32–39] and also to reports for several Cu alloys [32,33,40,41]. The results from Cu–Zn alloys [32,33] suggest that the rate of hardness evolution is dependent upon the stacking fault energy of the alloy and this is consistent also with other data suggesting a significant influence of stacking fault energy on the development of an ultrafine-grained structure both in HPT processing [42–49] and in processing by ECAP [50–53].

The gradual evolution towards homogeneity with increasing numbers of turns is visible for the Cu–0.1% Zr alloy both in the microhardness results and in the microstructural analysis. A lower hardness was introduced in the central region of the disk in the early stages of processing, equivalent to $N = 1/4$ turn in the present experiments, and this is attributed to the reduced shear strain in the central area as predicted by Eq. (1). Conversely, at the peripheral region the imposed strain is high and this leads to increased values of Hv. Thereafter, the lower hardness in the central region gradually sweeps outwards with increasing numbers of turns, as proposed earlier [4], until it occupies the total area of the disk as is evident at $N = 5$ turns in Fig. 2(c). Extending the torsional straining to $N = 10$ turns demonstrates complete homogenization and a constant value of Hv throughout the disk surface as shown in Fig. 2(d). Furthermore, these hardness values have negligible error bars as shown in the right column of Table 1.

As discussed recently, the present results showing the variation of hardness with the number of HPT turns, and therefore with the equivalent strain expressed by Eq. (1), depends in practice upon the nature of recovery in the material [16,54]. Most of the commercial purity metals and simple metallic alloys exhibit strain hardening in the initial stages of HPT processing. These types of metals, such as commercial purity Al and Al alloys [17,18,27,55] and Cu and Cu alloys [26,29,32–34,37], demonstrate lower hardness values at the centers of the disks in the early stages of deformation but with the hardness increasing with strain until ultimately there is a saturation value of Hv throughout each disk. This suggests the hardness homogeneity is evolving in the absence of any recovery due to the relatively low stacking fault energy. By contrast, a material such as high-purity aluminum has a very high stacking fault energy and this leads to easy cross-slip and rapid microstructural recovery [16] so that higher values of hardness are then recorded in the centers of the disks in the early stages of straining [16,56–58]. Moreover, very recent experiments showed that the situation is different for a material such as the Zn–Al eutectoid alloy where all of the measured hardness values were lower after HPT processing than the hardness values recorded in the annealed condition prior to processing [28,54]. This unique hardness distribution was attributed to the significant reduction in the distribution of the Zn precipitates in the Al-rich grains due to the high pressure applied to the disks during HPT processing [28,54]. There is evidence also for the development of local swirls and unusual shearing patterns in HPT processing in materials such as a two-phase Cu–Ag alloy [41,59,60], duplex stainless steel [61–63] and a magnesium AZ31 alloy [64].

The present results on the Cu–0.1% Zr alloy permit a direct comparison between the evolution of local hardness and the severely deformed microstructures in a series of disks. It is observed in the microhardness measurements that there are regions of lower hardness in the centers of the disks after processing at lower numbers of HPT revolutions and this is visible in the microstructures in the form of both the larger grains at the centers and the smaller grains at the edges of the disks after 1/4 and 1 turn as shown in Fig. 5(a) and (b). In the present experiments, reasonably homogeneous hardness and homogeneous microstructures were observed after 5 turns and the average grain size was then measured as ~180 nm in the peripheral region of the disk. These results are consistent with several other experiments. For example, a recent report on pure (99.97%) Cu processed at 6.0 GPa used electron backscatter diffraction (EBSD) to show the average grain size in the central region decreased with increasing numbers of turns and after 5 turns it was comparable to, but slightly larger than, the grain size of ~140 nm achieved in the peripheral region [29]. An identical grain size of ~140 nm was measured in the outer region of a pure (99.96%) Cu disk processed by HPT for 5 turns at 6.0 GPa [26] and a similar grain size of ~150 nm was reported in a Cu–1.49% Si alloy processed through 5 turns at 5.0 GPa [40].

4.2. Potential for achieving superplastic flow after HPT processing

The results in Fig. 4 show that the maximum tensile elongation recorded in these tests was ~280% for specimens processed through 5 and 10 turns of HPT and then tested at 723 K. This elongation is not within the regime of superplasticity which is formally defined as tensile elongations of at least 400% [65]. Nevertheless, it is significantly larger than the elongations of <100% recorded in tensile testing of a Cu–0.18% Zr alloy at 673 K after processing by ECAP [9]. The larger elongations in the present experiments are consistent with the smaller grain size of ~180 nm after HPT processing which compares with a grain size of ~350 nm after ECAP [9].

In practice, it is well known that the measured elongations in tensile testing are dependent upon the dimensions of the samples [66,67]. Specifically, tensile specimens having very small cross-sections are generally less ductile than larger specimens. In the present experiments, the gauge widths were only 1 mm and the gauge thicknesses were <0.8 mm after HPT processing so that the gauge sections were extremely small. By contrast, the earlier experiment on samples of the Cu–0.18% Zr alloy processed by ECAP used much larger gauge sections of 2 mm × 3 mm [9]. Nevertheless, despite the much larger size of the ECAP samples, the elongations to failure were significantly higher in the present experiments after processing by HPT. These higher elongations are due to the smaller grain size attained in HPT processing.

Finally, the elongations in the present experiments after HPT are much smaller than the record tensile elongation of ~1800% reported recently for a Zn–22% Al eutectoid alloy processed by HPT [68]. This confirm that, as concluded earlier for both Cu-based [9] and Al-based [69] alloys, the presence of a solid solution alloying element is an important prerequisite for achieving good superplastic elongations in tensile testing.

5. Summary and conclusions

1. A Cu–0.1% Zr alloy was processed by high-pressure torsion through up to a total of 10 turns under an applied pressure of 6.0 GPa. Experiments were conducted to examine the hardness evolution, the development of an ultrafine-grained microstructure and the tensile properties at elevated temperatures.
2. Processing by HPT reduces the grain size to ~180 nm at the edge of the disk after 5 turns. The measured hardness values are low in the central regions of the disks in the early stages of processing but there is a high level of hardness homogeneity after 5 and 10 turns. The hardness values are matched by microstructural observations showing a gradual evolution into a well-defined equiaxed grain structure.
3. Tensile testing at 673 and 723 K after 5 and 10 turns reveals a reasonable level of ductility but the alloy is not superplastic and the maximum elongation to failure is ~280% at 723 K using a strain rate of $1.0 \times 10^{-4}\,s^{-1}$.

Acknowledgement

This work was supported by the National Science Foundation of the United States under Grant No. DMR-0855009.

References

[1] R.Z. Valiev, T.G. Langdon, Prog. Mater. Sci. 51 (2006) 881.
[2] A.P. Zhilyaev, T.G. Langdon, Prog. Mater. Sci. 53 (2008) 893.
[3] A.P. Zhilyaev, B.K. Kim, G.V. Nurislamova, M.D. Baró, J.A. Szpunar, T.G. Langdon, Scr. Mater. 46 (2002) 575.
[4] A.P. Zhilyaev, G.V. Nurislamova, B.K. Kim, M.D. Baró, J.A. Szpunar, T.G. Langdon, Acta Mater. 51 (2003) 753.
[5] A.P. Zhilyaev, B.K. Kim, J.A. Szpunar, M.D. Baró, T.G. Langdon, Mater. Sci. Eng. A381 (2005) 377.
[6] M. Furukawa, Y. Iwahashi, Z. Horita, M. Nemoto, N.K. Tsenev, R.Z. Valiev, T.G. Langdon, Acta Mater. 45 (1997) 4751.
[7] H. Hasegawa, S. Komura, A. Utsunomiya, Z. Horita, M. Furukawa, M. Nemoto, T.G. Langdon, Mater. Sci. Eng. A265 (1999) 188.
[8] S. Lee, P.B. Berbon, M. Furukawa, Z. Horita, M. Nemoto, N.K. Tsenev, R.Z. Valiev, T.G. Langdon, Mater. Sci. Eng. A272 (1999) 63.
[9] K. Neishi, Z. Horita, T.G. Langdon, Mater. Sci. Eng. A352 (2003) 129.
[10] M. Goto, S.Z. Han, N. Kawagoishi, S.S. Kim, Mater. Lett. 62 (2008) 2832.
[11] M. Kawasaki, T.G. Langdon, Mater. Sci. Eng. A498 (2008) 341.
[12] G. Sakai, Z. Horita, T.G. Langdon, Mater. Sci. Eng. A393 (2005) 344.
[13] P. Serre, R.B. Figueiredo, N. Gao, T.G. Langdon, Mater. Sci. A528 (2011) 3501.
[14] A.P. Zhilyaev, S. Lee, G.V. Nurislamova, R.Z. Valiev, T.G. Langdon, Scr. Mater. 44 (2001) 2753.
[15] A.P. Zhilyaev, K. Oh-ishi, T.G. Langdon, T.R. McNelley, Mater. Sci. Eng. A410–411 (2005) 277.
[16] C. Xu, Z. Horita, T.G. Langdon, Acta Mater. 55 (2007) 203.
[17] A.P. Zhilyaev, T.R. McNelley, T.G. Langdon, J. Mater. Sci. 42 (2007) 1517.
[18] C. Xu, Z. Horita, T.G. Langdon, Acta Mater. 56 (2008) 5168.
[19] M. Kawasaki, B. Ahn, T.G. Langdon, J. Mater. Sci. 45 (2010) 4583.
[20] C. Xu, Z. Horita, T.G. Langdon, Mater. Trans. 51 (2010) 2.
[21] R.Z. Valiev, Yu.V. Ivanisenko, E.F. Rauch, B. Baudelet, Acta Mater. 44 (1996) 4705.
[22] F. Wetscher, A. Vorhauer, R. Stock, R. Pippan, Mater. Sci. Eng. A387–389 (2004) 809.
[23] F. Wetscher, R. Pippan, S. Sturm, F. Kauffmann, C. Scheu, G. Dehm, Metall. Mater. Trans. A 37A (2006) 1963.
[24] C. Xu, Z. Horita, T.G. Langdon, J. Mater. Sci. 43 (2008) 7286.
[25] A. Vorhauer, R. Pippan, Scr. Mater. 51 (2004) 921.
[26] Z. Horita, T.G. Langdon, Mater. Sci. Eng. A410–411 (2005) 422.
[27] C. Xu, T.G. Langdon, Mater. Sci. Eng. A503 (2009) 71.
[28] M. Kawasaki, B. Ahn, T.G. Langdon, Acta Mater. 58 (2010) 919.
[29] X.H. An, S.D. Wu, Z.F. Zhang, R.B. Figueiredo, N. Gao, T.G. Langdon, Scr. Mater. 63 (2010) 560.
[30] Z.C. Duan, X.Z. Liao, M. Kawasaki, R.B. Figueiredo, T.G. Langdon, J. Mater. Sci. 45 (2010) 4621.
[31] Y. Estrin, A. Molotnikov, C.H.J. Davies, R. Lapovok, J. Mech. Phys. Solids 56 (2008) 1186.
[32] T. Ungár, L. Balogh, Y.T. Zhu, Z. Horita, C. Xu, T.G. Langdon, Mater. Sci. Eng. A444 (2007) 153.
[33] L. Balogh, T. Ungár, Y. Zhao, Y.T. Zhu, Z. Horita, C. Xu, T.G. Langdon, Acta Mater. 56 (2008) 809.
[34] N. Lugo, N. Llorca, J.M. Cabrera, Z. Horita, Mater. Sci. Eng. A477 (2008) 366.
[35] K. Edalati, Z. Horita, Mater. Sci. Eng. A497 (2008) 168.
[36] K. Edalati, Y. Ito, K. Suehiro, Z. Horita, Int. J. Mater. Res. 100 (2009) 1668.
[37] K. Edalati, Z. Horita, Mater. Trans. 51 (2010) 1051.
[38] K. Edalati, Z. Horita, J. Mater. Sci. 45 (2010) 4578.
[39] J. Čížek, M. Janeček, O. Srba, R. Kužel, Z. Barnovská, I. Procházka, S. Dobatkin, Acta Mater. 59 (2011) 2322.
[40] H. Jiang, Y.T. Zhu, D.P. Butt, I.V. Alexandrov, T.C. Lowe, Mater. Sci. Eng. A290 (2000) 128.
[41] Y.Z. Tian, S.D. Wu, Z.F. Zhang, R.B. Figueiredo, N. Gao, T.G. Langdon, Acta Mater. 59 (2011) 2783.
[42] Y.H. Zhao, X.Z. Liao, Y.T. Zhu, Z. Horita, T.G. Langdon, Mater. Sci. Eng. A410–411 (2005) 188.
[43] Y.H. Zhao, Y.T. Zhu, X.Z. Liao, Z. Horita, T.G. Langdon, Appl. Phys. Lett. 89 (2006) 121906.
[44] Y.H. Zhao, Y.T. Zhu, X.Z. Liao, Z. Horita, T.G. Langdon, Mater. Sci. Eng. A463 (2007) 22.
[45] Y.H. Zhao, X.Z. Liao, Z. Horita, T.G. Langdon, Y.T. Zhu, Mater. Sci. Eng. A493 (2008) 123.
[46] Z.W. Wang, Y.B. Wang, X.Z. Liao, Y.H. Zhao, E.J. Lavernia, Y.T. Zhu, Z. Horita, T.G. Langdon, Scr. Mater. 60 (2009) 52.
[47] P.L. Sun, Y.H. Zhao, J.C. Cooley, M.E. Kassner, Z. Horita, T.G. Langdon, E.J. Lavernia, Y.T. Zhu, Mater. Sci. Eng. A525 (2009) 83.
[48] Y.B. Wang, X.Z. Liao, Y.H. Zhao, E.J. Lavernia, S.P. Ringer, Z. Horita, T.G. Langdon, Y.T. Zhu, Mater. Sci. Eng. A527 (2010) 4959.
[49] X.H. An, Q.Y. Lin, S.D. Wu, Z.F. Zhang, R.B. Figuiredo, N. Gao, T.G. Langdon, Scr. Mater. 64 (2011) 954.
[50] S. Komura, Z. Horita, M. Nemoto, T.G. Langdon, J. Mater. Res. 14 (1999) 4044.
[51] S. Qu, X.H. An, H.J. Yang, C.X. Huang, G. Yang, Q.S. Zang, Z.G. Wang, S.D. Wu, Z.F. Zhang, Acta Mater. 57 (2009) 1586.
[52] X.H. An, Q.Y. Lin, S. Qu, G. Yang, S.D. Wu, Z.F. Zhang, J. Mater. Res. 24 (2009) 3636.
[53] X.H. An, Q.Y. Lin, S.D. Wu, Z.F. Zhang, Mater. Sci. Eng. A527 (2010) 4510.
[54] M. Kawasaki, B. Ahn, T.G. Langdon, Mater. Sci. Eng. A527 (2010) 7008.
[55] A. Loucif, R.B. Figueiredo, T. Baudin, F. Brisset, T.G. Langdon, Mater. Sci. Eng. A527 (2010) 4864.
[56] Y. Ito, Z. Horita, Mater. Sci. Eng. A503 (2009) 32.
[57] K. Edalati, Z. Horita, Mater. Trans. 50 (2009) 92.
[58] M. Kawasaki, R.B. Figueiredo, T.G. Langdon, Acta Mater. 59 (2010) 308.
[59] Y.Z. Tian, X.H. An, S.D. Wu, Z.F. Zhang, R.B. Figueiredo, N. Gao, T.G. Langdon, Scr. Mater. 63 (2010) 65.
[60] Y.Z. Tian, S.D. Wu, Z.F. Zhang, R.B. Figueiredo, N. Gao, T.G. Langdon, Mater. Sci. Eng. A528 (2011) 4331.

[61] Y. Cao, Y.B. Wang, S.N. Alhajeri, X.Z. Liao, W.L. Zheng, S.P. Ringer, T.G. Langdon, Y.T. Zhu, J. Mater. Sci. 45 (2010) 765.
[62] Y. Cao, M. Kawasaki, Y.B. Wang, S.N. Alhajeri, X.Z. Liao, W.L. Zheng, S.P. Ringer, Y.T. Zhu, T.G. Langdon, J. Mater. Sci. 45 (2010) 4545.
[63] Y. Cao, Y.B. Wang, R.B. Figueiredo, L. Chang, X.Z. Liao, M. Kawasaki, W.L. Zheng, S.P. Ringer, T.G. Langdon, Y.T. Zhu, Acta Mater. 59 (2011) 3903.
[64] R.B. Figueiredo, T.G. Langdon, Mater. Sci. Eng. A528 (2011) 4500.
[65] T.G. Langdon, J. Mater. Sci. 44 (2009) 5998.
[66] Y.H. Zhao, Y.Z. Guo, Q. Wei, A.M. Dangelewicz, C. Xu, Y.T. Zhu, T.G. Langdon, Y.Z. Zhou, E.J. Lavernia, Scr. Mater. 59 (2008) 627.
[67] Y.H. Zhao, Y.Z. Guo, Q. Wei, T.D. Topping, A.M. Dangelewicz, Y.T. Zhu, T.G. Langdon, E.J. Lavernia, Mater. Sci. Eng. A525 (2009) 68.
[68] M. Kawasaki, T.G. Langdon, Mater. Sci. Eng. A528 (2011) 6140.
[69] M. Furukawa, A. Utsunomiya, K. Matsubara, Z. Horita, T.G. Langdon, Acta Mater. 49 (2001) 3829.